

Full Coulomb calculation of Stark broadening in laser-produced plasmas

L. A. Woltz* and C. F. Hooper, Jr.

Physics Department, University of Florida, Gainesville, Florida 32611

(Received 25 August 1983)

The full Coulomb interaction between radiating ions and perturbing electrons is included in the calculation of Lyman-series spectral line profiles emitted by highly ionized hydrogenic radiators in a dense, hot plasma. Profiles from this calculation and from a similar calculation based on the dipole approximation for the radiator-perturber interaction are compared over a range of plasma densities. The significance of inelastic collisions between the radiator and perturbing electrons is also examined.

I. INTRODUCTION

In the past few years the plasma-broadened spectral lines of highly ionized high- Z elements have been used as a diagnostic for the plasma conditions obtained in laser-driven pellet implosion experiments.¹⁻⁶ Since the plasmas in some recent experiments have reached densities for which the average electron spacing approaches the size of the radiating ions, the dipole approximation for the radiator-perturber interaction, which many theoretical line-shape calculations have used, has become of questionable validity. In this work we extend the line-shape formalism of Tighe and Hooper,⁷⁻⁹ which was based on the dipole approximation, by retaining the full-Coulomb interaction between the radiating ions and the perturbing electrons of the plasma. We will neglect terms of higher order than dipole in the radiator-perturbing ion interaction. This approximation is much better for the ions than for the electrons in the case of high- Z perturbers since the ion density is $1/Z_{\text{ion}}$ times the electron density and since the large ion-radiator repulsion tends to keep the ions and radiators apart. However, for high-density deuterium-tritium plasmas with a small amount of high- Z impurity, terms of higher order than dipole in the radiator-ion interaction may have a significant effect on the line shape.

We compare the profiles calculated with the full-Coulomb treatment of Ar XVIII Lyman line profiles with those calculated using a dipole approximation over a range of plasma densities to assess the validity of the dipole approximation. We compare Lyman- α and - β line profiles from this full-Coulomb formalism with those from a full-Coulomb formalism developed by Griem *et al.*,¹⁰ which is based on quantum-mechanical distorted-wave calculations. The profiles used in this comparison include only elastic electron-radiator collisions,¹¹ but the calculations of Griem *et al.* can also include inelastic collisions. We also consider broadening effects due to inelastic electron collisions.

II. FORMALISM

The line-shape function, in the static ion approximation, is given by¹²

$$I(\omega) = \int_0^\infty P(\epsilon) J(\omega, \epsilon) d\epsilon, \quad (1)$$

where $P(\epsilon)$ is the ion microfield probability distribution,^{13,14}

$$J(\omega, \epsilon) = \frac{1}{\pi} \text{Re} \text{Tr}_{re} \int_0^\infty e^{i\omega t} \vec{d} \cdot \rho_{re} e^{-iH(\epsilon)t/\hbar} \vec{d} e^{iH(\epsilon)t/\hbar} dt \quad (2)$$

is the electron-broadened line profile for a radiating ion in the presence of the ion microfield $\vec{\epsilon}$, Tr_{re} is a trace over radiator and electron states, \vec{d} is the radiator dipole operator, ρ_{re} is the density operator for the radiator and perturbing electrons, and $H(\epsilon)$ is given by

$$\begin{aligned} H(\epsilon) &= H_r + e\epsilon z_r + H_e + V_{er} \\ &= H(r) + H_e + V_{er}. \end{aligned} \quad (3)$$

Here, H_r is the unperturbed Hamiltonian for the radiator, z_r is the z coordinate of the radiating electron, H_e is the Hamiltonian for the plasma electrons, V_{er} is the radiator-electron interaction, and $H(r)$ is the Hamiltonian for the radiator in the presence of the static ion field. For convenience we have chosen the z axis to be in the direction of the static ion field. We also take the radiator nucleus to be the origin of our coordinates. Corrections to the static ion approximation are discussed elsewhere.¹⁵ In Eq. (1) Doppler broadening of the line shape due to radiator motion has been neglected. This will be included approximately at the end of the calculation by convolving $I(\omega)$ with a Doppler profile based on a Maxwell velocity distribution.

Employing well-known transform techniques^{7,8,16} and neglecting any plasma-generated static level shifts, which are believed to be small, we can write Eq. (2) as

$$J(\omega, \epsilon) = -\frac{1}{\pi} \text{Im} \text{Tr}_r \vec{d} \cdot [\omega - L(r) - M(\omega)]^{-1} f(r) \vec{d}, \quad (4)$$

where

$$f(r) = e^{-\beta H(r)} / \text{Tr}_r e^{-\beta H(r)}, \quad (5)$$

with $\beta \equiv 1/k_B T$. The Liouville operator $L(r)$ represents a commutator of the corresponding Hamiltonian,

$$L(r)g(r) = [H(r), g(r)]. \quad (6)$$

In this work we will restrict the width and shift operator $M(\omega)$ (which contains the average electron-broadening effects) to second order in the radiator-perturbing electron interaction $V_1(r,1)$, where $V_{er} = \sum_i V_1(r,i)$. Initially we will also neglect interactions between perturbing electrons; the correlation effects thus neglected will be reintroduced in an approximate manner later in the calculation. The neglect of perturbing electron interactions permits us to write the electron Hamiltonian as a sum of single-particle Hamiltonians,

$$H_e = \sum_i H(i). \quad (7)$$

Since the radiator is at the origin of our coordinate system, the long-range monopole part of the interaction between the radiator and one perturbing electron, $-(Z-1)e^2/x_1$, is a function only of the perturber's coordinate, \vec{x}_1 . Therefore, we include it in the one-electron Hamiltonian $H(1)$ by redefining $H(1)$ and $V_1(r,1)$ as

$$H(1) = \frac{p_1^2}{2m} - \frac{(Z-1)e^2}{x_1} \quad (8)$$

and

$$V_1(r,1) = \frac{e^2}{|\vec{x}_r - \vec{x}_1|} - \frac{e^2}{x_1}. \quad (9)$$

We can now expand $M(\omega)$ in the short-ranged potential $V_1(r,1)$, while retaining to all orders the effect of the radiator monopole on the perturbing electrons. The eigenfunctions of the Hamiltonian $H(1)$ for the perturbing electrons are the Coulomb wave functions.¹⁷ Use of these wave functions in a second-order, low-frequency calculation of $M(\omega)$ corresponds to the Coulomb-Born approximation.

For plasma conditions and Lyman lines which we will consider, a large part of each line satisfies the condition $\Delta\omega \lesssim \omega_{pe}$, where $\Delta\omega$ is the frequency separation from line center and ω_{pe} is the electron plasma frequency. The electron broadening of this part of the line is primarily due to weak electron collisions, so we can well approximate $M(\omega)$ by retaining only second-order terms in an expansion in $V_1(r,1)$.¹⁸ Another indication that strong collisions (those which cannot be accurately treated by a second-order theory) should not be too significant here can be seen from Fig. 1. There we compare the x_1 dependence of a radiator matrix element of the dipole part ($l=1$ part of a spherical harmonic expansion) of the Coulomb interaction to the x_1 dependence of the corresponding matrix element of the dipole interaction, which is proportional to $1/x_1^2$. The dipole part of the Coulomb interaction differs from the dipole interaction in that the radiator is not treated as a point dipole; rather the perturbing electrons encounter a much softer potential due to the finite extent of the radiator wave function. A strong collision cutoff formula given by Griem *et al.*¹⁰ for straight-line path classical electrons and a point dipole radiator indicates that for 800-eV electrons the electron-radiator impact parameter would have to be ≤ 0.13 times the actual radius of the radiator ($n^2 a_0/Z$) for a collision to be strong. Figure 1 shows that the dipole part of the Coulomb interaction is everywhere less than the dipole

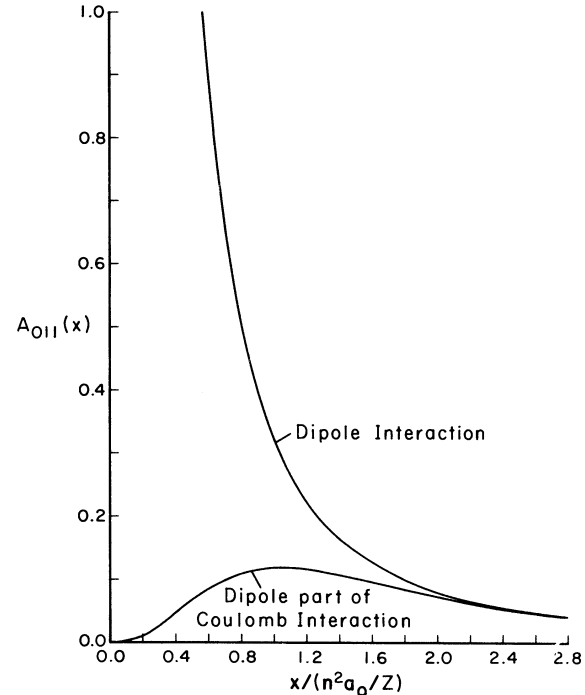


FIG. 1. Comparison of the dipole part of the Coulomb interaction, $\langle 21 | (x_-/x_+^2) | 20 \rangle = A_{011}(x)$ [see Eq. (16)], with the dipole interaction, $\langle 21 | (x_r/x^2) | 20 \rangle$. Here, $\langle x | nl \rangle$ represents the radial part of the hydrogenic wave function.

potential evaluated at this cutoff (this remains true when the other weaker multipoles of the full-Coulomb interaction are included), so most electron collisions, even most of those which penetrate the radiator, should be accurately represented here by a second-order form of $M(\omega)$. With the above approximations, $M(\omega)$ takes the form

$$M(\omega) = n_e \text{Tr}_1 L_1(r,1) [\omega - L(r) - L(1)]^{-1} L_1(r,1) f(1), \quad (10)$$

where Tr_1 is a trace over states of one perturbing electron, n_e is the electron density, and

$$f(1) = \frac{N}{n_e} e^{-\beta H(1)} / \text{Tr}_1 e^{-\beta H(1)}. \quad (11)$$

Here we will calculate Lyman series lines so we neglect lower state broadening. If we also assume that perturbing electrons do not cause the radiator to undergo nonradiative transitions between states of different principal quantum number (no-quenching approximation) and neglect Stark shifts of higher than first order due to the ion microfield, we can write $M(\omega)$ in the matrix form⁸

$$[M(\omega)]_{ii'} = - \frac{in_e}{\hbar^2} \text{Tr}_1 \int_0^\infty dt \sum_{i''} e^{i\Delta\omega t} V_{ii''} e^{-iH(1)t/\hbar} \times V_{i''i} e^{iH(1)t/\hbar} f(1), \quad (12)$$

where $\Delta\omega = \omega - (E_{i''} - E_f)/\hbar$, the subscript i (f)

represents initial (final) states for the particular Lyman line to be calculated, and $V_{ii'}$ is the radiator matrix element of $V_1(r,1)$. The significance of inelastic collisions neglected in the no-quenching approximation is considered later in this paper.

This form of $M(\omega)$ with the dipole approximation for

$V_1(r,1)$ was used by O'Brien¹⁹ and Tighe^{7,8} in calculating Lyman line shapes for charged radiators. However, we expand the full-Coulomb interaction, $V_1(r,1)$, in spherical harmonics and use Coulomb wave functions to evaluate the trace in Eq. (12). This gives for the real and imaginary parts of $M(\omega)$ (Ref. 20)

$$M_R(\Delta\omega) = \frac{1}{\hbar^2} \int_0^\infty dk_1 \int_0^\infty dk_2 e^{-\beta\hbar^2 k_1^2/2m} \frac{G(k_1, k_2) - G\left[k_1, \left[k_1^2 + \frac{2m\Delta\omega}{\hbar}\right]^{1/2}\right]}{\Delta\omega + \frac{\hbar}{2m}(k_1^2 - k_2^2)}, \quad \Delta\omega > 0 \quad (13)$$

$$M_I(\Delta\omega) = -\frac{m\pi}{\hbar^3} \int_0^\infty dk_1 e^{-\beta\hbar^2 k_1^2/2m} \frac{G\left[k_1, \left[k_1^2 + \frac{2m\Delta\omega}{\hbar}\right]^{1/2}\right]}{\left[k_1^2 + \frac{2m\Delta\omega}{\hbar}\right]^{1/2}}, \quad \Delta\omega > 0 \quad (14)$$

and similar equations for $\Delta\omega < 0$. The term $G(k_1, k_2)$ is given by

$$G_{n l_1 m_1, n l_2 m_2}(k_1, k_2) = \frac{4n_e \lambda_T^3 e^4}{\pi^2} \delta_{l_1 l_2} \delta_{m_1 m_2} \sum_{l_3=0}^{n-1} \sum_{l_5=0}^{2n-2} \sum_{l_4, l_6=0}^{\infty} \frac{(2l_3+1)(2l_4+1)(2l_6+1)}{2l_5+1} \\ \times \begin{bmatrix} l_1 & l_3 & l_5 \\ 0 & 0 & 0 \end{bmatrix}^2 \begin{bmatrix} l_4 & l_5 & l_6 \\ 0 & 0 & 0 \end{bmatrix}^2 \\ \times \left[\int_0^\infty dx F_{l_4}(\eta_1, k_1 x) F_{l_6}(\eta_2, k_2 x) A_{l_1 l_3 l_5}(x) \right]^2, \quad (15)$$

where

$$A_{l_1 l_3 l_5}(x) = \int_0^\infty dx_r x_r^2 R_{n l_1}(x_r) \\ \times \left[\frac{x_{<}^{l_5}}{x_{>}^{l_5+1}} - \frac{\delta_{l_5,0}}{x} \right] R_{n l_3}(x_r), \quad (16)$$

$F_l(\eta, kx)$ is the Coulomb wave function,¹⁸ $R_{nl}(x_r)$ is the hydrogenic radial wave function of the radiator, and $x_{<}$ ($x_{>}$) is the lesser (greater) of x_r and x , the radial coordinates of the radiator electron and perturbing electron. The l_3 sum is over initial radiator angular momenta, the l_5 sum is over multipoles of the Coulomb interaction, and the l_4 and l_6 sums are over perturber angular momenta. Equation (16) gives the x dependence of multipoles of the radiator-perturber interaction. The symbol

$$\begin{bmatrix} l_1 & l_2 & l_3 \\ m_1 & m_2 & m_3 \end{bmatrix}$$

is the Wigner 3- j symbol.

Increasing values of l_4 and l_6 in the function $G(k_1, k_2)$ correspond to increasing separation of the radiator and perturber; so for l_4 and l_6 greater than some value, say l' , we can use the dipole approximation for the radiator-perturber interaction with negligible error. Use of the dipole approximation simplifies the l_4 and l_6 sums to a form which can be done exactly from $l'+1$ to infinity.²¹

We evaluate the electron broadening operator $M_I(\Delta\omega)$ numerically from Eqs. (14)–(16), then use these results in

Eqs. (4) and (1) to generate line profiles. The effect of $M_R(\Delta\omega)$ on the line appears to be small²⁰ and we will neglect it here.

In obtaining Eqs. (14)–(16) for $M_I(\Delta\omega)$, we neglected electron-electron interactions, and thus the effects of electron-electron correlations. These correlations, which produce a screening of the radiator-perturbing electron interaction, most significantly affect that part of the line shape corresponding to times long compared to electron relaxation times, i.e., for frequencies inside the electron plasma frequency ω_{pe} .²² Smith²³ and Hussey *et al.*²² have shown that the inclusion of correlations has little effect on $M_I(\Delta\omega)$ for $|\Delta\omega| > \omega_{pe}$ and that for $|\Delta\omega| < \omega_{pe}$ the correlated result for $M_I(\Delta\omega)$ is nearly equal to the uncorrelated result evaluated at the plasma frequency, $M_I(\omega_{pe})$. Hence, to approximate the effects of correlations on $M_I(\Delta\omega)$, we set $M_I(\Delta\omega) = M_I(\omega_{pe})$ for $|\Delta\omega| \leq \omega_{pe}$.

III. RESULTS

Figures 2 and 3 show Lyman- α line profiles calculated for a plasma of Ar¹⁷⁺ ions and electrons at densities of 10^{24} and 10^{25} electrons/cm³ and a temperature of 800 eV. Figures 4 and 5 show Lyman- β lines and Figs. 6 and 7 show Lyman- γ lines for the same plasma densities and temperature. Each figure contains profiles calculated with (1) our full-Coulomb formalism, (2) a similar formalism in which the dipole approximation for the radiator-

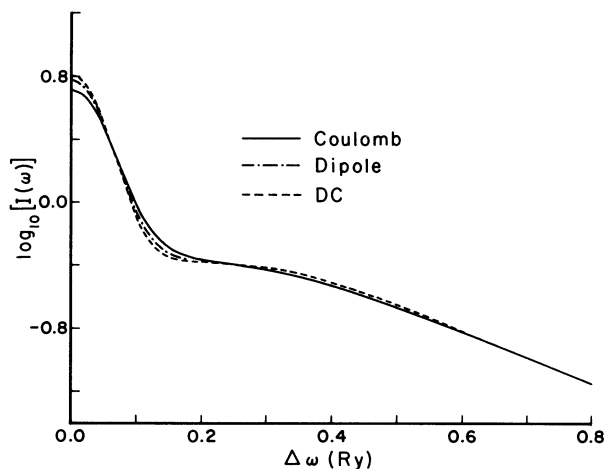


FIG. 2. Argon Lyman- α line profiles calculated with the Coulomb interaction, the dipole interaction, and the dipole part of the Coulomb interaction (DC). The density is equal to 10^{24} electrons/cm 3 and the temperature is 800 eV.

perturbing electron interaction is used,^{7,8} and (3) from the dipole part of the Coulomb interaction: l_3 is restricted to equal 1 in Eq. (15). The fine-structure splitting, which we have neglected here but will include in a later paper, causes a large asymmetry in the Lyman- α profiles; so the Lyman- α profiles should only be used for comparison of the various calculations. The fine-structure splitting also causes a significant asymmetry in Lyman- β profiles at lower densities ($\lesssim 10^{23}$ cm $^{-3}$).

As was discussed previously, the dipole interaction overestimates the actual dipole part of the Coulomb radiator-perturbing electron interaction for perturbers near the radiator; this results in line profiles which are broader than those calculated from the dipole part of the Coulomb interaction. A measure of this overestimate comes from a comparison of line profiles calculated from the dipole part of the Coulomb interaction with those pro-

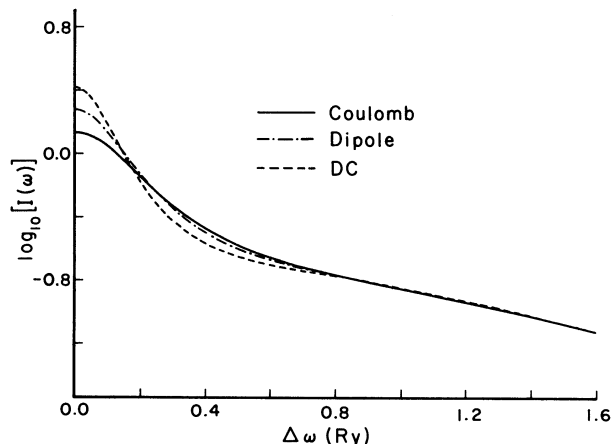


FIG. 3. Same as Fig. 2 but at a density of 10^{25} electrons/cm 3 .

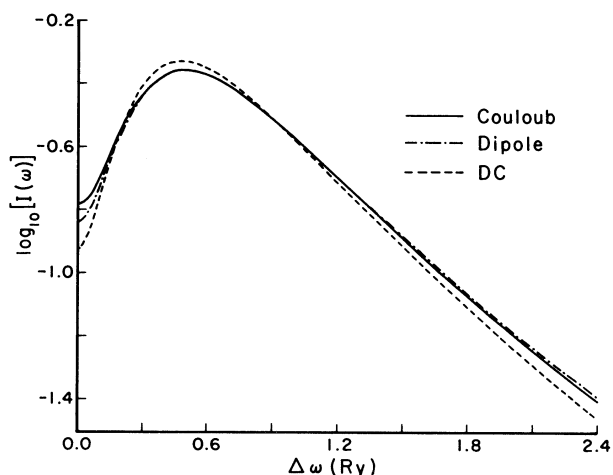


FIG. 4. Argon Lyman- β line profiles calculated with the Coulomb interaction, the dipole interaction, and the dipole part of the Coulomb interaction (DC). The density is equal to 10^{24} electrons/cm 3 and the temperature is 800 eV.

files calculated from the dipole interaction. These, in turn, can be compared with full-Coulomb profiles to determine the significance that the $l=0,2,3, \dots, 2n-2$ multipoles have in broadening the lines.

The difference between profiles calculated from the dipole approximation and from the dipole part of the Coulomb interaction is small at 10^{23} electrons/cm 3 but increases as the density increases; and the greater the principal quantum number of the initial radiator state, the greater the difference.

The difference between line profiles calculated from the full-Coulomb interaction and from the dipole part of the Coulomb interaction is small at 10^{23} electrons/cm 3 but increases as the density increases; the increase becomes progressively larger in going from the α to the γ line. Although we have explicitly removed a long-range monopole contribution from $V_1(r,1)$ [see Eq. (9)], the redefined expression for $V_1(r,1)$ contains a monopole term that is sig-

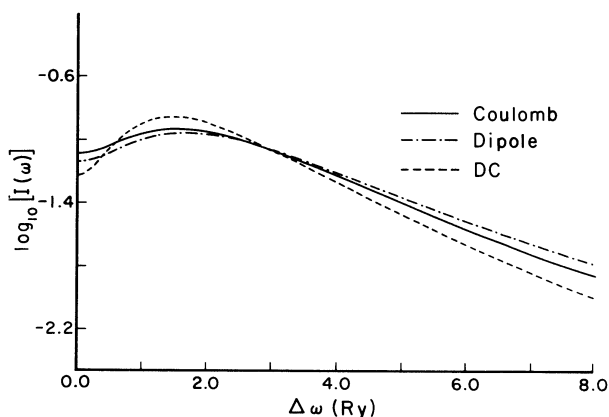


FIG. 5. Same as Fig. 4 but at a density of 10^{25} electrons/cm 3 .

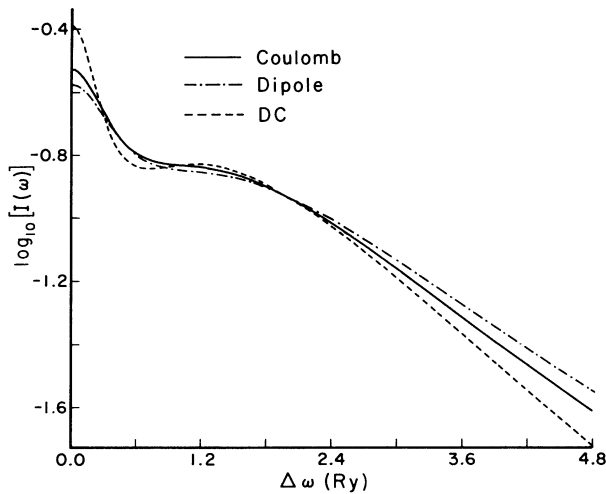


FIG. 6. Argon Lyman- γ line profiles calculated with the Coulomb interaction, the dipole interaction, and the dipole part of the Coulomb interaction (DC). The density is equal to 10^{24} electrons/cm 3 and the temperature is 800 eV.

nificant only when the perturber penetrates the radiator. This short-range monopole contribution to the interaction is largely responsible for the difference between the calculations based on the Coulomb interaction and on the dipole part of the Coulomb interaction. The contribution from the higher multipoles ($l_5=2,3,\dots,2n-2$) is almost negligible for Lyman α and causes a slight but noticeable broadening of the β and γ lines, which increases with the density.

It is interesting to note that even for fairly high densities, the calculation using the dipole interaction can give line profiles which are fortuitously close to those from the

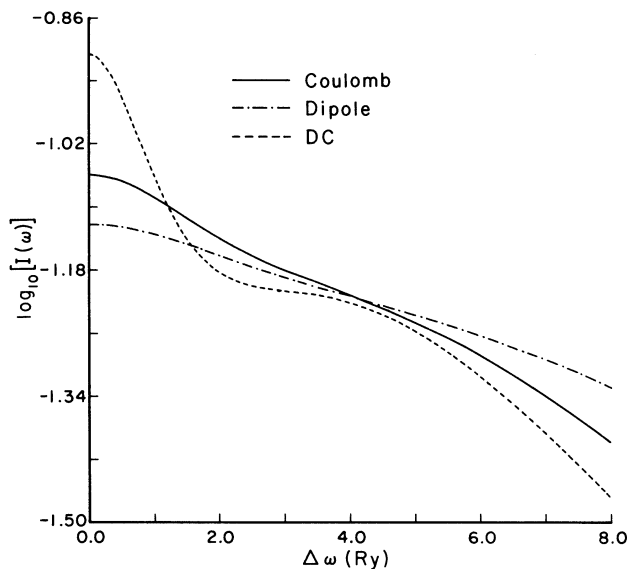


FIG. 7. Same as Fig. 6 but at a density of 10^{25} electrons/cm 3 .

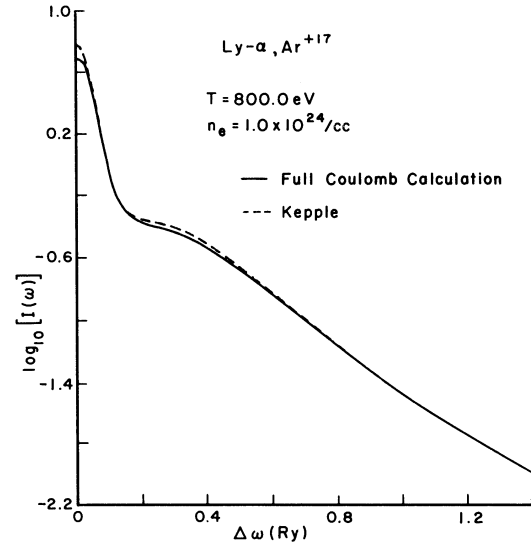


FIG. 8. Comparison of argon Lyman- α line profiles calculated from this full-Coulomb formalism and from the full-Coulomb formalism of Griem, Blaha, and Kepple. The density is equal to 10^{24} electrons/cm 3 and the temperature is 800 eV.

full-Coulomb calculation (e.g., the Lyman- β line at 10^{24} /cm 3 and 800 eV).

In Figs. 8 and 9 we compare Lyman- α and - β line shapes calculated from this full-Coulomb relaxation theory to corresponding line shapes calculated from a full-Coulomb formalism of Griem *et al.*^{10,11} which includes, by a method based on distorted-wave scattering cross sections, the quantum-mechanical effects of close electron-radiator collisions. Figures 8 and 9 show that

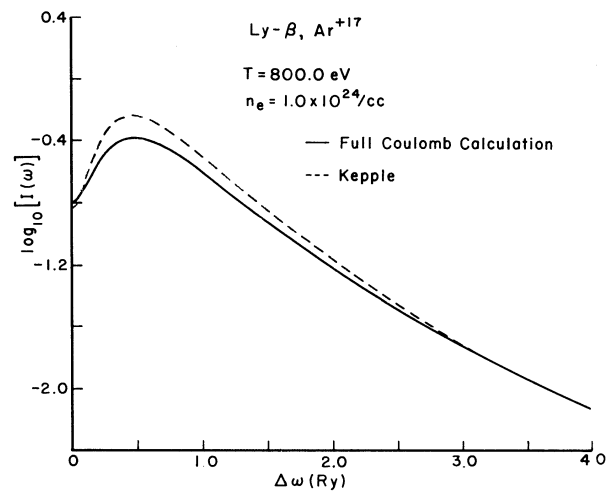


FIG. 9. Comparison of argon Lyman- β line profiles calculated from this full-Coulomb formalism and from the full-Coulomb formalism of Griem, Blaha, and Kepple. The density is equal to 10^{24} electrons/cm 3 and the temperature is 800 eV.

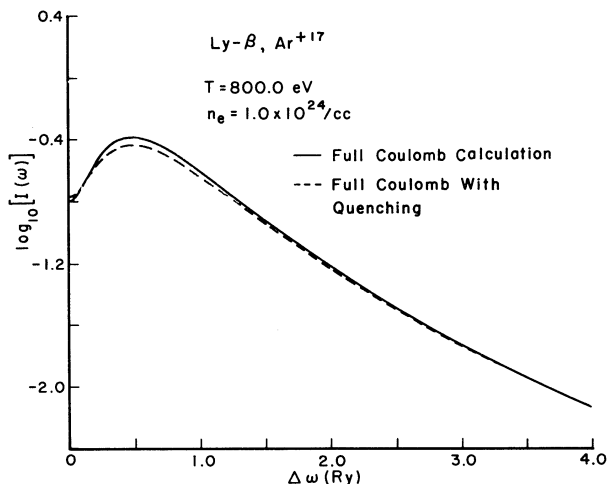


FIG. 10. Comparison of argon Lyman- β line profiles calculated with (solid line) and without (dashed line) radiator-perturbing electron interaction matrix elements between radiator states of principal quantum number 3 and 4. The density is equal to 10^{24} electrons/cm 3 and the temperature is 800 eV.

our α and β lines are slightly broader than lines of Griem *et al.* which include elastic collisions that penetrate the radiator. In this range of plasma conditions our calculation, when used to determine experimental plasma densities, would indicate a density about 18% lower than would the calculation of Griem *et al.*

In the calculation of the profiles shown in Figs. 2–9 we have assumed that matrix elements of the radiator-perturber interactions between radiator states having different principal quantum numbers are negligible; and we have set them equal to zero, thus neglecting inelastic electron collisions.

To determine the significance of the neglected matrix elements, we have calculated Lyman- β line profiles in which states having principal quantum numbers 4 and 5 have been included in the set i'' in $M(\omega)$ [Eq. (12)]. Figure 10 shows that inclusion of the states with $n=4$ gives a small but noticeable additional broadening. The inclusion of states with $n=4$ and 5 causes only a slight fur-

ther broadening. States having higher principal quantum numbers will have an even smaller effect; so Fig. 10 should well represent the additional broadening due to inelastic collisions.

IV. SUMMARY

In this work we have extended the line-shape formalism of Tighe and Hooper^{7–9} by eliminating the dipole approximation that they used for the radiator-perturbing electron interaction, retaining instead the full-Coulomb interaction; and we have compared Coulomb and dipole calculations of Ar XVIII Lyman line profiles over a range of plasma densities pertinent to current laser implosion experiments. We find that for a density of 10^{23} electrons/cm 3 and a temperature of 800 eV the two calculations agree well for Lyman- α , - β , and - γ lines. At 10^{24} electrons/cm 3 the agreement is not quite as good; but it is better than might be expected considering that the average electron separation is on the order of the radiator size. This near agreement is a fortuitous consequence of the dipole approximation giving an overestimate of the actual dipole part of the Coulomb interaction for perturbers near the radiator, partially compensating for broadening due to the multipoles neglected in that approximation. The agreement becomes worse in going to higher lines of the series. At 10^{25} electrons/cm 3 there is a significant difference between the α lines and a large difference between the β lines and the γ lines. A comparison of our line profiles with those calculated by Griem *et al.*^{10,11} shows a fair agreement, with our profiles being slightly broader.

We have also included the effects of inelastic radiator-perturbing electron collisions in the calculation of a Lyman- β line, obtaining a slightly broader β line profile than when the inelastic collisions are neglected.

ACKNOWLEDGMENTS

This work was supported by the U. S. Department of Energy (Lawrence Livermore National Laboratory—Laser Fusion Program) under Contract No. DE-AS08-81DP40159-MOD1.

*Present address: Atomic and Plasma Radiation Division, National Bureau of Standards, Washington, D.C. 20234.

¹B. Yaakobi, D. Steel, E. Thorsos, A. Hauer, and B. Perry, Phys. Rev. Lett. **39**, 1526 (1977).

²B. Yaakobi *et al.*, Phys. Rev. A **19**, 1247 (1979).

³B. Yaakobi *et al.*, Phys. Rev. Lett. **44**, 1072 (1980).

⁴J. D. Kilkenny, R. W. Lee, M. H. Key, and J. G. Lunney, Phys. Rev. A **22**, 2746 (1980).

⁵J. P. Apruzese, P. C. Kepple, K. G. Whitney, J. Davis, and D. Duston, Phys. Rev. A **24**, 1001 (1981).

⁶A. Hauer *et al.*, Phys. Rev. Lett. **45**, 1495 (1980).

⁷R. J. Tighe and C. F. Hooper, Jr., Phys. Rev. A **14**, 1514 (1976).

⁸R. J. Tighe, Ph.D. thesis, University of Florida, 1977.

⁹R. J. Tighe and C. F. Hooper, Jr., Phys. Rev. A **17**, 410 (1978).

¹⁰H. R. Griem, M. Blaha, and P. C. Kepple, Phys. Rev. A **19**, 2421 (1979).

¹¹P. C. Kepple (private communication).

¹²H. R. Griem, *Spectral Line Broadening by Plasmas* (Academic, New York, 1974).

¹³C. F. Hooper, Jr., Phys. Rev. **165**, 215 (1968).

¹⁴R. J. Tighe and C. F. Hooper, Jr., Phys. Rev. A **15**, 1773 (1977).

¹⁵R. Cauble and H. R. Griem, Phys. Rev. A **27**, 3187 (1983).

¹⁶T. W. Hussey, J. W. Dufty, and C. F. Hooper, Jr., Phys. Rev. A **12**, 1084 (1975).

¹⁷M. Abramowitz and I. A. Stegun, *Handbook of Mathematical Functions* (Dover, New York, 1972).

¹⁸E. W. Smith, J. Cooper, and C. R. Vidal, Phys. Rev. **185**, 140 (1969).

¹⁹J. T. O'Brien, Ph.D. thesis, University of Florida, 1970.

²⁰L. A. Woltz, Ph.D. thesis, University of Florida, 1982.

²¹L. C. Biedenharn, Phys. Rev. **102**, 262 (1956).

²²T. W. Hussey, J. W. Dufty, and C. F. Hooper, Jr., Phys. Rev. A **16**, 1248 (1977).

²³E. W. Smith, Phys. Rev. **166**, 102 (1968).